Chromic Oxide Recovery from Tannery Wastewater and Application as Dye

Medina, Carlos[1]; Debut, Alexis[2]; Silva, Jorge[1]; Gallegos, Julio[1]; Vicuña, Kerlyn[1]; Palmay, Paúl[1]; Carrera, Santiago[1,*]

[1]Escuela Superior Politécnica de Chimborazo, Facultad de Ciencias, Riobamba, Ecuador
[2]Universidad de las Fuerzas Armadas ESPE, Centro de Nanociencia y Nanotecnología, Sangolquí, Ecuador

Abstract: The leather tanning industry utilizes large amounts of chromium in its processes, resulting in substantial volumes of wastewater that contain high concentrations of chromium. This wastewater could serve as a source for recovering this metal after disposal. This study aims to exploit this wastewater to extract chromium oxide (Cr_2O_3), a material with a wide range of useful properties suitable for various applications. In this study, the effluent was used as a chromium (III) source, and ammonium hydroxide (NH_4OH) was employed as a precipitant, adjusting the pH to 10. The resulting precipitate was filtered, dried at 70°C, and then calcined at 400, 600, and 700°C for 5 hours. After calcination, the material was ground for a further analysis. Characterization of the material was performed using Fourier Transform Infrared (FT-IR) spectroscopy, X-ray Diffraction (XRD), and Scanning Electron Microscopy with Energy Dispersive X-ray Spectroscopy (SEM-EDX). FT-IR analysis revealed characteristic peaks corresponding to chromium oxide (III). XRD studies confirmed the formation of Cr_2O_3 with a hexagonal structure. SEM images indicated that the particles lacked a defined shape, with crystal sizes varying between 25 and 97 µm and an average crystal size of 78 nm. The presence of chromium oxide was further confirmed through EDS compositional analysis.

Keywords: chromic oxide, dye, wastewater, precipitating agent

Recuperación de Óxido Crómico a Partir de Aguas Residuales de Curtiduría y Aplicación como Colorante

Resumen: La industria del curtido de pieles utiliza grandes cantidades de cromo en su proceso, lo que da lugar a grandes volúmenes de aguas residuales con altas concentraciones de cromo. Éstas podrían ser una fuente para la recuperación de este metal tras su eliminación. El objetivo de este estudio es aprovechar estas aguas residuales para la extracción de óxido de cromo (Cr_2O_3), un material con una amplia gama de propiedades que puede utilizarse en numerosas aplicaciones. En el estudio, se utilizaron efluentes como fuente de cromo (III) e hidróxido de amonio (NH_4OH) como precipitante hasta un pH de 10. El precipitado resultante se filtró, y se secó a 70°C y luego se calcinó a 400, 600 y 700°C durante 5 h. A continuación, el precipitado se molió para un análisis más detallado. El material se caracterizó por infrarrojo con transformada de Fourier (FT-IR), difracción de rayos X (DRX) y microscopía electrónica de barrido (SEM-EDX). El análisis FTIR reveló picos característicos de óxido de cromo (III). Los estudios de DRX confirmaron la formación de Cr_2O_3 con estructura hexagonal. Las imágenes SEM mostraron que las partículas no tenían una forma definida. El tamaño de los cristales variaba entre 25 y 97 µm, con un tamaño medio de 78 nm. La presencia de óxido de cromo se confirmó mediante análisis de composición EDS.

Palabras clave: óxido crómico, colorante, agua-residual, agente precipitante

1. INTRODUCTION

The development of the tanning industry in Ecuador has been driven by the growing market for leather products such as handbags, belts, shoes, and jackets. These industries generate wastewater contaminated with a significant concentration of chromium (Zhao & Chen, 2019) that has not fully reacted during the leather tanning process. The increase in leather production generates significant amounts of wastewater. This metal can be recovered through chemical reactions. However, if the water is not properly treated, it becomes an environmental problem.

Tanning is an industry whose main activity consists of subjecting animal skins, mainly bovine and ovine, to chemical treatments using chromium salts (Zhou et al., 2018). These processes aim to modify leather to obtain a material that is hardly waterproof, durable, soft, and flexible (Nashy et al.,

*luissantiago.carrera@espoch.edu.ec
Recibido: 17/04/2024
Aceptado:15/01/2025
Publicado en línea: 28/02/2025

10.33333/rp.vol55n1.04
CC 4.0

2012; Wang et al., 2022b). Over time, many methods of hide preservation have been perfected, but the use of chromium salts, such as $Cr(OH)SO_4$, in the tanning process has always remained the industrial standard. This approach guarantees a product that does not deteriorate under different environmental conditions. It also protects against the degrading action of microorganisms such as fungi, insects, and other microscopic life forms (Rathore, 2015).

Chromium is a highly toxic pollutant, especially in its hexavalent (IV) state, which forms chromates, dichromates, and acids. The total chromium concentration limit for industrial effluents is 1 mg/L. There are significant risks to humans, including a high risk of cancer, dermatitis, nephritis, and respiratory problems, from elevated levels of chromium (III) or (VI) in water (Kirti Shekhawat, Sreemoyee Chatterjee, 2015; Tumolo et al., 2020). It also leads to contamination of soil, water, and air (Shore & Shemesh, 2016; Zhao & Chen, 2019). Although the trivalent form of chromium is considered to be less toxic and more stable, it can be converted to its hexavalent form in the presence of oxidizing agents, for example, oxygen in the air or other oxides (Chávez, 2010).

Therefore, it is essential to explore various strategies for the recovery of residual chromium, such as chemical precipitation, ion exchange, reverse osmosis, or adsorption processes (Minas et al., 2017). Recovery by precipitation and subsequent thermal treatment to convert it into Cr_2O_3, a useful product that can reduce its environmental impact, is a promising route for its utilization. Because of the problems associated with the direct discharge of chromium into the environment, this study aims to take advantage of the high concentrations of chromium present in the wastewater. Chromium levels in tanning industry water may be as high as 1300-8000 mg/L (Minas et al., 2017), especially in small-scale industries in countries where there are no environmental regulations to control the discharge of contaminated water.

An important alternative to reduce waste and reduce direct and indirect effluent contamination is the recovery of the chromium salts used in the process. The obtained chromium (III) hydroxide is subjected to high temperatures to facilitate the fragmentation of the particulates and to obtain the corresponding oxide (Huang et al., 2016). Cr_2O_3 has remarkable properties, including high hardness, low friction, high wear resistance, corrosion resistance, and good optical properties (Golosova et al., 2017). These properties enable a wide range of applications, such as protective coatings, optical and electronic applications, solar energy protective films for windows (Zhao et al., 2018a), catalysts (Yin et al., 2019), dyes and pigments (Tsegay et al., 2022), solar energy applications (Tsegay et al., 2022) and sunscreens (Talavari et al., 2018).

As mentioned above, trivalent chromium oxide is a compound with a wide range of industrial applications. This green solid is used as a pigment in the production of emerald green paint for glass and ceramics. In the manufacture of glass, the green color is achieved by combining cobalt, zinc, and chromium oxides during the melting of the glass. When the glass cools, the green color is obtained (Chua et al., 2022). In ceramics, the colorant is added in powder form to the frits. The frits are then fired at high temperatures to achieve the desired color (Gayo & Lavat, 2018). Calcined Cr_2O_3 can be used in coatings for various materials. In addition to its solubility in water, it contains chromophores that give the characteristic green color to various industrial paints (Wang et al., 2022a; Zhang et al., 2014). Catalysts, on the other hand, are substances that speed up reactions without changing the chemical composition of the elements involved, thus obtaining optimum results without affecting the reaction as a whole (Gao et al., 2019; Zhang et al., 2022). These include chromium and iron metal oxides used in hydrocarbon processing.

The main objective of this work is to develop a simple method for the synthesis of Cr_2O_3 particles by aqueous precipitation with ammonia as a precipitant (Huang et al., 2016). This approach involves an economical one-step synthesis process. The use of ammonium hydroxide is targeted due to its high solubility and the generation of alkaline conditions (pH > 11) by the formation of OH^- ions (Zhang et al., 2014). However, the possibility of using other bases, such as sodium hydroxide or calcium hydroxide is not excluded.

In this research, chromium oxide was synthesized to be used as a colorant. Precipitation-calcination processes were applied using wastewater from the tannery industry. Calcination was carried out at three different temperatures: 400, 600, and 800º C. The Cr_2O_3 is characterized by various analytical techniques, including X-ray diffraction (XRD), scanning electron microscopy (SEM-EDX) coupled with energy-dispersion spectrometry (EDX), and Fourier transform infrared (FT-IR). This oxide can be reused as a colorant in the glass industry, in paints, in jewelry, and as a corrosion inhibitor.

2. METHODOLOGY

2.1 Chromium oxide synthesis using synthetic water

Solutions of industrial-grade basic chromium sulfate [$Cr(OH)SO_4$] at a concentration of 0.2 mol/L and a 96% solution of ammonium hydroxide (NH_4OH) were prepared. A volume of 500 mL of the $Cr(OH)SO_4$ solution was placed in three beakers, and aqueous NH_4OH was added dropwise while stirring constantly at 120 rpm until pH values of 9, 10, and 11 were achieved in each experiment. The samples were allowed to stand for 24 h, after which the precipitate was removed via vacuum filtration. The filtered material was then dried at 70°C for 24 h. Finally, the dried samples were calcined at 400 °C, 600 °C, and 800 °C for 5 h in each experiment and then crushed.

2.2 Synthesis of chromium oxide using wastewater

The method used for the extraction of chromium oxide from synthetic water will be replicated. Place 500 mL of tannery wastewater in a beaker. Add aqueous NH_4OH drop by drop with constant stirring (120 rpm) until pH = 10. The samples are allowed to stand for 24 h, then vacuum filtered and dried at 70°C for 24 h. Finally, the dried samples are calcined at 400, 600, and 800°C for 5 h and then crushed.

2.3 Determination of chromium concentration in wastewater

Using atomic absorption spectrophotometry, the concentration of total chromium in the tannery effluent is calculated both

before and after chromium oxide synthesis. The percentage of chromium removed from the water is calculated from these data. Acidify the samples with nitric acid (HNO_3) to a pH below 2 to avoid chromium precipitation and preserve its soluble form. Heat the samples and add hydrogen peroxide (H_2O_2) to oxidize organic compounds that may interfere. For the calibration curve, chromium standard solutions are prepared using potassium dichromate ($K_2Cr_2O_7$).

Total chromium is determined by the Standard Methods 3111 B direct air-acetylene flame method. A Perkin Elmer AAnalyst200X atomic absorption spectrometer is used. It is equipped with a chromium-specific hollow cathode lamp at a wavelength of 357,9 nm. An air/acetylene mixture is used with flow rates of 11.5L/min for air and 6.5 L/min for acetylene.

2.4 Characterization of chromic oxide

The Cr_2O_3 dye samples were characterized by Fourier transform infrared spectroscopy (FTIR) using a JASCO FT/IR-100 model spectrophotometer. This analysis allows the detection of possible organic remnants of the tanning process present in the sample, in addition to the identification of the chromium oxide. Scanning electron microscopy with a field emission gun (FEG-SEM) is used to study the morphology of the particles, their size distribution, and composition. The instrument used is a TESCAN model MIRA3. The compositional analysis is performed by an energy dispersive spectroscopy (EDX) with a BRUKER XFlash 6130 detector. The resolution is 123 eV for Mn alpha. A double adhesive layer of carbon tape is used on the sample holders during the SEM analysis. A 20-nanometer gold layer is applied using a QUORUM Q150R sputter coater to ensure the conductivity of the samples. X-ray diffraction (XRD) is used to determine the crystal structure parameters and the crystal structure of the Cr_2O_3 dye crystals. The analysis was performed with a PANalytical Empyrean diffractometer in θ-2θ configuration (Bragg-Brentano geometry), equipped with a Cu X-ray tube (Kα radiation λ = 1.54056 Å) operating at 40 kV and 40 mV.

3. RESULTS AND DISCUSSION

3.1 Synthesis of Cr_2O_3 dye samples

To evaluate the effectiveness of the precipitant with the mass of precipitate, the experimental phase of this research began with the preparation of synthetic water samples. This will determine the optimum pH to be used in the experiments with the tannery effluent sample. The selection of the appropriate pH value is based on the amount of precipitate that is obtained from synthetic water. Dry precipitate masses of 3.87 g, 4.79 g, and 4.22 g are obtained for pH 9, 10, and 11, respectively. However, the masses of precipitate at different pH did not show scattered values. It was found that samples treated at pH 10 produced more precipitates, so this pH (10) was chosen for further studies with tanning water.

In addition, the initial and final measurements of the total chromium content in the wastewater were carried out to determine the percentage of chromium removal. These concentrations are 315 and 164 mg/L, respectively. This indicates that 47.94% of the chromium originally present in the water was removed.

Tanning wastewater contains a complex mixture of contaminants including heavy metals and organic compounds like grease and oil. The presence of these compounds can form emulsions. This makes them difficult to separate and affects the precipitation of chromium. Furthermore, the ions present can interact and form complexes, making chromium separation difficult. Normally, wastewater has an acidic pH of about 3.5. The solubility of the trivalent chromium (Cr(III)) is favored, but it is difficult to precipitate it as $Cr(OH)_3$. For effective precipitation, therefore, pretreatment to remove organic matter is required.

Although 100% removal of chromium from the wastewater was not obtained, this process could be used as a preliminary step before applying specific treatments, such as filter absorption or ion exchange, to remove the maximum amount of chrome so that the wastewater can be discharged into the sewer system.

For example, the recovery of chromium by precipitation with NaOH and $Ca(OH)_2$ achieved a removal of 99.9%, starting from an initial concentration of 5000 mg/L of chromium in the water of a tannery (Murgueitio et al., 2015). Likewise, the removal of chromium by chemical precipitation with lime and cement achieves a removal of 97% from an initial concentration of 2350 mg/L of chromium (Engy et al., 2016). Similarly, 98% removal was achieved in 2 h of treatment with water containing 3250 mg/L of total chromium using lime and cement in combination with biological treatment (Hesham & Engy, 2016). Moreover, using water from a tannery with 2000 mg/L chromium, 99.7% of chromium was removed from wastewater by a chemical process using NaOH and electrochemical treatment (Mella et al., 2016).

3.2 Characterization of the dye with FTIR

Characteristic peaks at 536 and 613 cm^{-1} are observed in the FT-IR spectra in Figure 1 corresponding to the oxide prepared from synthetic water (standard sample) and calcined at 800ºC. These peaks indicate the presence of Cr_2O_3 crystals which give transmissions below 1000 cm^{-1} and are indicative of stretching of the O-Cr-O bond.

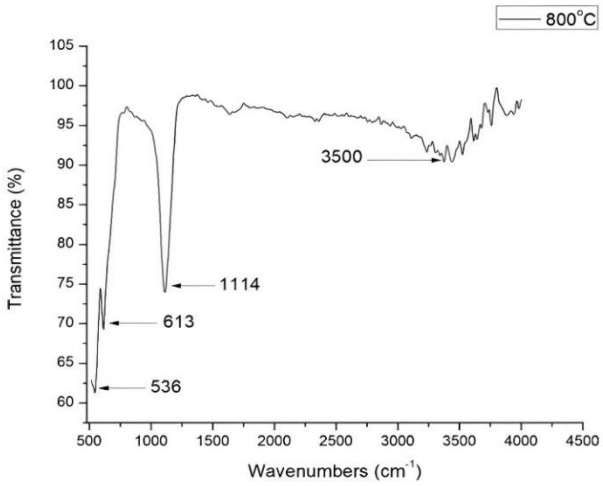

Figure 1. FT-IR spectra obtained for the synthetic water samples (standard samples) were calcined at 800ºC

The FT-IR spectra in Figure 2 show the absorptions of metal oxides. Absorption bands below 1000 cm^{-1} are due to interatomic vibrations (Kamari et al., 2019). The sample calcined at 400ºC shows peaks at 506 and 520 cm^{-1}, characteristic of O-Cr-O bond stretching, indicating the presence of Cr_2O_3 crystals (Abdullah et al., 2014). The sample calcined at 600º C shows a lower percentage of transmittance with peaks due to stretching of the M-O (O-Cr-O) bond at 506 and 519 cm^{-1}.

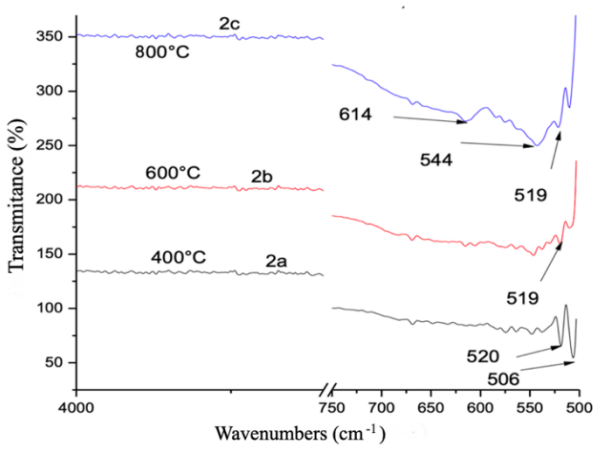

Figure 2. FT-IR spectra were obtained at calcination temperatures of 400, 600, and 800ºC

The sample calcined at 800ºC shows a higher transmission percentage and peaks, indicating the stretches of the M-O (Cr-O) bond at 519, 544, and 614 cm^{-1}, confirming the formation of Cr-O bonds in the chromium oxide (Gibot, 2020; Zhang et al., 2014).

3.3 SEM-EDS morphological analysis

Figure 3 shows the sample synthesized using synthetic water at pH 10, which was then calcined between 400 and 800 °C. The image shows that the sample contains particles with sizes ranging from 0.303 to 0.521 mm. The particles have irregular shapes and large sizes. EDS spectra show the presence of chromium, oxygen, and other elements such as calcium, chlorine, sulfur, and aluminum.

Morphology and compositional analyses are carried out by scanning electron microscopy coupled with energy-dispersive spectroscopy. Samples synthesized at pH 10 and calcined at 400, 600, and 800 °C are shown in Figure 3. The micrograph of the samples at 400 °C, with particle sizes ranging from 28 to 97 mm, is shown in Figure 3a. Samples calcined at 600°C, Figure 3b, show sizes between 25 and 44mm. Finally, the samples calcined at 800 °C with particle sizes ranging from 33 to 76 mm are shown in Figure 3c. All micrographs show that the Cr_2O_3 dye particles do not have a defined or uniform morphology (Wang et al., 2019; Yahyazadehfar et al., 2020). In addition, it is observed that as the temperature increases, the size of the particles decreases, but the agglomeration of the particles is quite noticeable in all the cases.

In the EDS spectra in Figure 3, in addition to chromium and oxygen, distinct peaks can be seen. These peaks indicate the presence of elements such as calcium, chlorine, sulfur, aluminum, magnesium, and sodium. It is assumed that these elements were present as co-precipitated ions in the synthesis process. They probably originated from the products used in the tanning process and were still in solution in the effluent. All of the samples show a distinct peak at 5.8 keV, which corresponds to the presence of chromium oxide (Abdullah et al., 2014; Kadowaki et al., 2018). However, the EDS spectrum of the sample treated at 800ºC shows 9.232% by mass. This is higher than the 6.409% and 7.599% of the samples treated at 400ºC and 600ºC, respectively. Furthermore, faint peaks corresponding to other oxides (CaO, $Al2O_3$, MgO, Na_2O) are present in the sample, as shown in Figure 3 (Zhao et al., 2018b).

Figure 4 shows the X-ray diffraction (XRD) pattern of the Cr_2O_3 dye obtained from synthetic water. The dye was calcined at 800°C. The presence of impurities is responsible for the observed non-indexed peaks, which do not correspond to the crystal structure of Cr_2O_3. The non-indexed peaks observed, which do not correspond to the crystal structure of Cr_2O_3, are attributed to the presence of impurities. During $Cr(OH)_3$ formation, these impurities co-precipitate in the solid phase and on calcination also produce oxides reflected in the diffraction pattern. Comparing the XRDs of the standard with those obtained from the effluent, the presence of Miller indexes (104) and (202) are observed in both diffraction patterns, confirming the presence of Cr_2O_3, in addition to other oxides.

3.4 XRD analysis

X-ray diffraction (XRD) patterns of Cr_2O_3 dyes calcined at different temperatures are shown in Figure 5. The indexed peaks correspond to the crystal structure planes of chromium oxide with lattice parameters a=4.953 Å, b=4.953 Å, c=13.588 Å and angles α=90º, β=90º, γ=120º. These parameters are indicative of a compact hexagonal crystal structure with a cell volume of 288.69 pm^3 (Cao & Zuo, 2017). As confirmed in Table 1 of the EDX spectra, the non-indexed peaks observed, which are not consistent with the crystal structure of Cr_2O_3, are due to the presence of impurities. In addition to Cr^{3+}, other cations have been identified which form oxides and can distort the diffraction pattern of the pure dye. The morphological properties of the dyes, analyzed by Cu-Kα radiation (wavelength 1.5406 Å) in the 2θ range (10-80º), show clearly distinguishable peaks of higher intensity at angles 32.60, 46.30 and 57.80, corresponding to Miller indices (104), (202) and (018), which support the crystalline structure of Cr_2O_3 (Wang et al., 2018). Using these three peaks as a reference, an average crystal size of 78 nm is estimated using the Debye-Scherrer equation (Afzal et al., 2016; Gibot, 2020; Wang et al., 2019). In addition, the intensities of the indexed peak (104) at temperatures of 400, 600 and 800ºC, are 12249.478, 7429.045 and 18415.296 respectively. This confirms more Cr_2O_3 at 800ºC, corresponding to the highest intensity obtained.

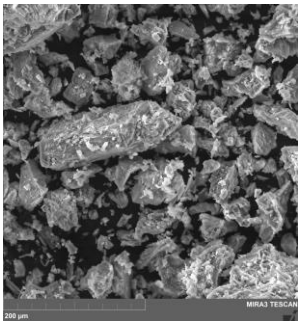

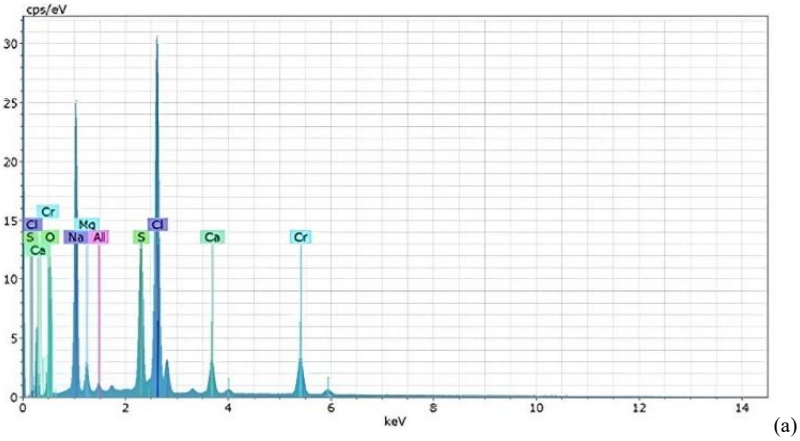

(a)

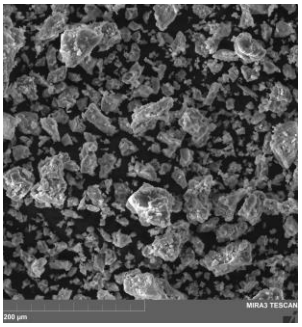

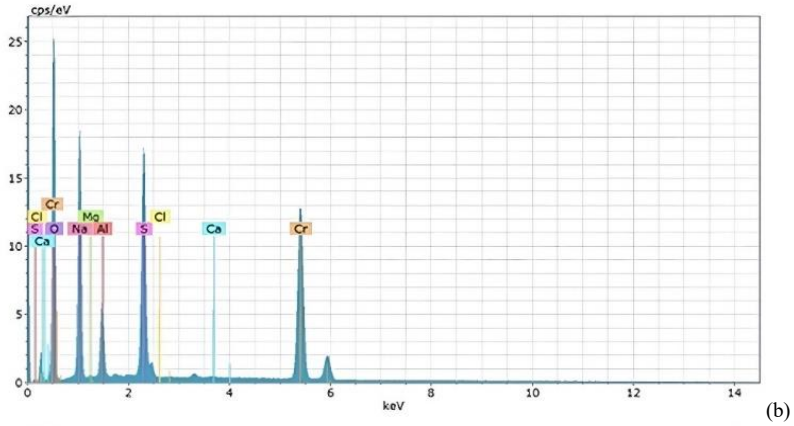

(b)

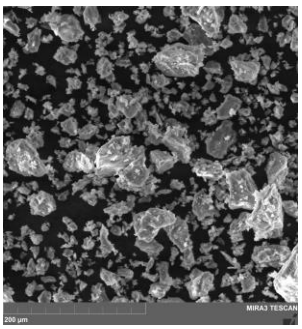

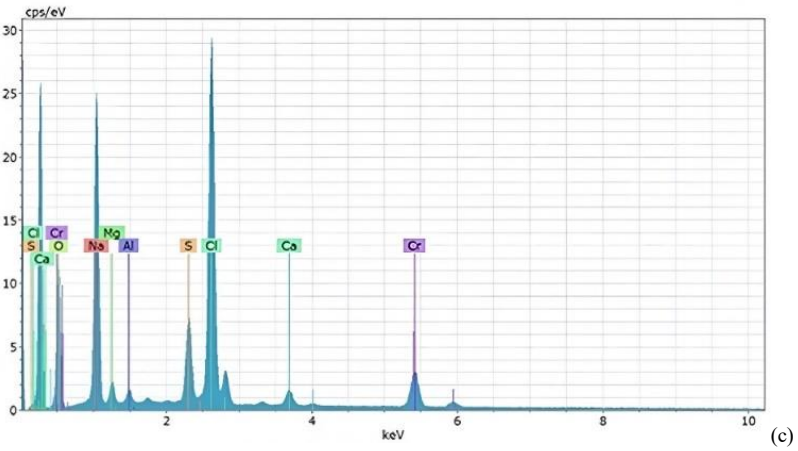

(c)

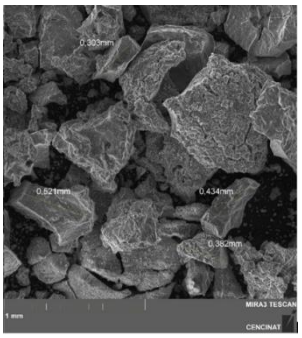

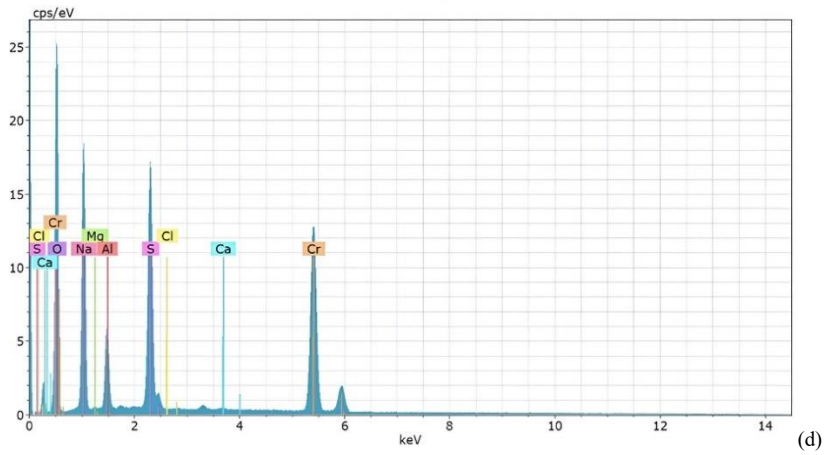

(d)

Figure 3. SEM micrographs of wastewater sample calcined at (a) 400ºC, (b) 600ºC, (c) 800ºC and (d) (standard sample) calcined at 800°C

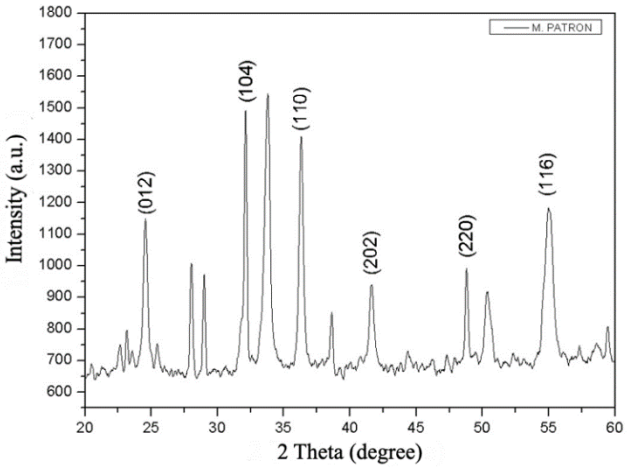

Figure 4. The diffractogram of synthetic water sample (standard sample) calcined at 800ºC

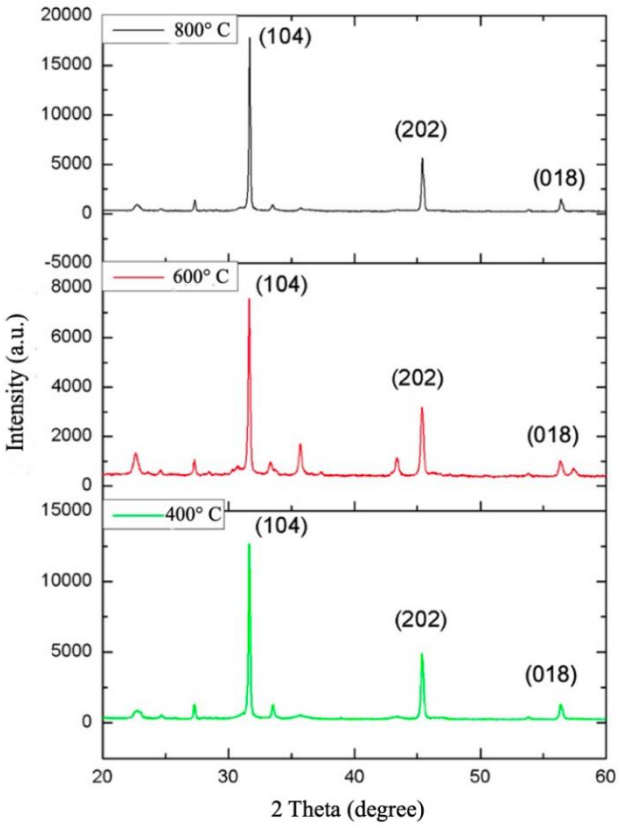

Figure 5. Diffractograms of the samples calcined at 400, 600, and 800°C

Table 1. Composition analysis expressed in mass % of samples at pH 10 and different calcination temperatures

Element	% Mass			
	400ºC	600ºC	800ºC	Standard Sample 800ºC
Oxygen	41.188	35.007	38.099	42.893
Sodium	21.201	24.169	24.995	16.967
Magnesium	1.791	1.485	4.435	0.104
Aluminum	0.092	0.634	0.241	3.377
Sulfur	5.878	5.368	4.535	11.133
Chlorine	21.369	23.695	17.032	0.000
Calcium	2.069	2.045	1.436	0.115
Chromium	6.409	7.599	9.232	25.415

3.5 Staining test

The staining test evaluated the effect of the dye and was carried out on a fragment of glazed glass that had been melted at 900°C. Figure 1(a) shows a green tint, but further experiments are needed to improve the distribution of the tint across the glass surface. Furthermore, other tests should also be carried out with different percentages of Cr_2O_3 added to the glass during the melting process. According to the literature, it is indicated that the chromium oxide, as a refractory pigment, should be in the range of 1 – 3 % by mass in order to obtain an optimum green color. Similarly, the dye dissolved in water was used in staining tests on canvas and porcelain-based reliefs. Figure 6 shows(b) an optinal green staining.

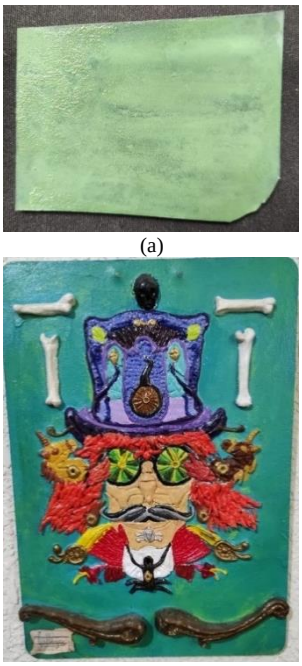

(a)

(b)

Figure 6. Staining tests (a) on glass and (b) on canvas

4. CONCLUSIONS

Precipitation proves to be a straightforward process with significant potential for remediating the environment. The recovery of chromium (III) oxide from wastewater is its main advantage. This is an excellent coloring agent for various materials. Characterization of the recovered material confirms that the particles correspond to Cr_2O_3. The FTIR shows a characteristic stretching of this oxide. Furthermore, morphological analysis by SEM-EDS shows that the particles do not have a defined shape and have sizes below 76 µm when calcined at 800°C. This is the temperature that gives the best results in this study. Despite the co-precipitation of other oxides identified in the compositional analysis, the Cr_2O_3 content is predominant at 13% by mass. XRD analyses confirm the presence of chromium oxide, showing the characteristic peaks of the compound and its hexagonal crystalline structure. The results will provide a basis for future research into the recovery and re-use of toxic chemicals for the environment, such as chromium (VI).

REFERENCES

Abdullah, M. M., Rajab, F. M., & Al-Abbas, S. M. (2014). Structural and optical characterization of Cr2O3 nanostructures: Evaluation of its dielectric properties. *AIP Advances*, *4*(2), 0–11. https://doi.org/10.1063/1.4867012

Afzal, A., Atiq, S., Saleem, M., Ramay, S. M., Naseem, S., & Siddiqi, S. A. (2016). Structural and magnetic phase transition of sol–gel-synthesized Cr2O3 and MnCr2O4 nanoparticles. *Journal of Sol-Gel Science and Technology*, *80*(1), 96–102. https://doi.org/10.1007/s10971-016-4066-4

Cao, Z., & Zuo, C. (2017). Cr2O3/carbon nanosheet composite with enhanced performance for lithium ion batteries. *RSC Advances*, *7*(64), 40243–40248. https://doi.org/10.1039/c7ra06188a

Chávez, A. (2010). Descripción de la nocividad del cromo proveniente de la industria curtiembre y de las posibles formas de removerlo. *Revista Ingenierías*, *9*(17), 41–49. http://www.redalyc.org/articulo.oa?id=75017164003

Chua, L., Quan, S. Z., Yan, G., & Yoo, W. S. (2022). Investigating the Colour Difference of Old and New Blue Japanese Glass Pigments for Artistic Use. *J. Conserv. Sci*, *38*(1), 1–13. https://doi.org/10.12654/JCS.2022.38.1.01

Engy, A., Hesham, A., Amr, M., & D, A. (2016). Remediation and recycling of chromium from tannery wastewater using combined chemical – biological treatment system. *Process Safety and Environmental Protection*, *104*, 1–10. https://doi.org/10.1016/j.psep.2016.08.004

Gao, X.-Q., Lu, W.-D., Hu, S.-Z., Li, W.-C., & Lu, A.-H. (2019). Rod-shaped porous alumina-supported Cr2O3 catalyst with low acidity for propane dehydrogenation. *Chinese Journal of Catalysis*, *40*(2), 184–191. https://doi.org/https://doi.org/10.1016/S1872-2067(18)63202-4

Gayo, G. X., & Lavat, A. E. (2018). Green ceramic pigment based on chromium recovered from a plating waste. *Ceramics International*, *44*(18), 22181–22188. https://doi.org/https://doi.org/10.1016/j.ceramint.2018.08.336

Gibot, P. (2020). Centimetric-sized chromium (III) oxide object synthesized by means of the carbon template replication. *Ceramics*, *3*(1), 92–100. https://doi.org/10.3390/ceramics3010010

Golosova, N. O., Kozlenko, D. P., Kichanov, S. E., Lukin, E. V., Liermann, H. P., Glazyrin, K. V., & Savenko, B. N. (2017). Structural and magnetic properties of Cr2O3 at high pressure. *Journal of Alloys and Compounds*, *722*, 593–598. https://doi.org/10.1016/j.jallcom.2017.06.140

kirtiHuang, Z., Chen, C., Xie, J., & Wang, Z. (2016). The evolution of dehydration and thermal decomposition of nanocrystalline and amorphous chromium hydroxide. *Journal of Analytical and Applied Pyrolysis*, *118*, 225–230. https://doi.org/10.1016/j.jaap.2016.02.006

Kadowaki, H., Katasho, Y., Yasuda, K., & Nohira, T. (2018). Electrolytic Reduction of Solid Al 2 O 3 to Liquid Al in Molten CaCl 2 . *Journal of The Electrochemical Society*, *165*(2), D83–D89. https://doi.org/10.1149/2.1191802jes

Kamari, H. M., Al-Hada, N. M., Baqer, A. A., Shaari, A. H., & Saion, E. (2019). Comprehensive study on morphological, structural and optical properties of Cr2O3 nanoparticle and its antibacterial activities. *Journal of Materials Science: Materials in Electronics*, *30*(8), 8035–8046. https://doi.org/10.1007/s10854-019-01125-2

Mella, B., Glanert, A. C. C., & Mariliz, G. (2013). *Removal of chromium from tanning wastewater by chemical precipitation and electrocoagulation* (Vol. 100). https://doi.org/10.1016/j.psep.2015.03.007

Minas, F., Singh Chandravanshi, B., & Leta, S. (2017). Chemical precipitation method for chromium removal and its recovery from tannery wastewater in Ethiopia. *Chemistry International*, *3*(4), 291–305. Retrieved from www.bosaljournals/chemint/editorci@bosaljournals.com

Murgueitio, E., Pinto, W., & Landivar, J. (2015). REMOVAL FROM SYNTHETIC WATER LEVEL LABORATORY , USING LAYERED DOUBLE HYDROXIDES (HDL). *Revista de La Sociedad Química Del Perú*, *81*(2).

Nashy, E. H. A., Osman, O., Mahmoud, A. A., & Ibrahim, M. (2012). Molecular spectroscopic study for suggested mechanism of chrome tanned leather. *Spectrochimica Acta - Part A: Molecular and Biomolecular Spectroscopy*, *88*, 171–176. https://doi.org/10.1016/j.saa.2011.12.024

Rathore, D. S. (2015). Study of fungal Diversity on different types of Finished Leather and Leather Articles. *Research Journal of Recent Sciences*

Shahid, M., Shamshad, S., Rafiq, M., Khalid, S., Bibi, I., Niazi, N. K., … Rashid, M. I. (2017). Chromium speciation, bioavailability, uptake, toxicity and detoxification in soil-plant system: A review. *Chemosphere*, *178*, 513–533. https://doi.org/10.1016/j.chemosphere.2017.03.074

Shore, L. S., & Shemesh, M. (2016). Estrogen as an Environmental Pollutant. *Bulletin of Environmental Contamination and Toxicology*, *97*(4), 447–448. https://doi.org/10.1007/s00128-016-1873-9

Talavari, F., Shakeri, A., & Mighani, H. (2018). Synthesis of Cr2O3/TiO2 Nanocomposite and its Application as the Blocking Layer in Solar Cells. *Journal of Environmental Analytical Chemistry*, *05*(01), 2–6. https://doi.org/10.4172/2380-2391.1000231

Tsegay, M. G., Gebretinsae, H. G., G.Welegergs, G., Maaza, M., & Nuru, Z. Y. (2022). Novel green synthesized Cr2O3 for selective solar absorber: Investigation of structural, morphological, chemical, and optical properties. *Solar Energy*, *236*, 308–319. https://doi.org/https://doi.org/10.1016/j.solener.2022.03.011

Tumolo, M., Ancona, V., De Paola, D., Losacco, D., Campanale, C., Massarelli, C., & Uricchio, V. F. (2020). Chromium pollution in European water, sources, health risk, and remediation strategies: An overview. *International Journal of Environmental Research and Public Health*, *17*(15), 1–25. https://doi.org/10.3390/ijerph17155438

Wang, F., He, N., Li, H., Ji, L., Liu, X., Ye, Y., … Chen, J. (2018). Mechanical and tribological properties of Cr/Cr2O3 multilayer films. *Proceedings of the Institution of Mechanical Engineers, Part J: Journal of Engineering Tribology*, *232*(10), 1195–1202. https://doi.org/10.1177/1350650117743683

Wang, H., Han, W., Li, X., Liu, B., Tang, H., & Li, Y. (2019). Solution combustion synthesis of Cr2O3 nanoparticles and the catalytic performance for dehydrofluorination of 1,1,1,3,3-pentafluoropropane to 1,3,3,3-tetrafluoropropene. *Molecules*, *24*(2), 1–12. https://doi.org/10.3390/molecules24020361

Wang, Xinyan, Ju, P., Lu, X., Chen, Y., & Wang, F. (2022a). Influence of Cr2O3 particles on corrosion, mechanical and thermal control properties of green PEO coatings on Mg alloy. *Ceramics International*, *48*(3), 3615–3627. https://doi.org/https://doi.org/10.1016/j.ceramint.2021.10.142

Wang, Xuechuan, Lan, X., Zhu, X., & Sun, S. (2022b). Preparation of a ricinoleic acid modified amphoteric polyurethane for leather cleaner and simplifying production. *Journal of Cleaner Production*, *330*, 129877. https://doi.org/https://doi.org/10.1016/j.jclepro.2021.129877

Yahyazadehfar, M., Ahmadi, S. A., Sheikhhosseini, E., & Ghazanfari, D. (2020). High-yielding strategy for microwave-assisted synthesis of Cr2O3 nanocatalyst. *Journal of Materials Science: Materials in Electronics*, *31*(14), 11618–11623. https://doi.org/10.1007/s10854-020-03710-2

Yin, Y., Li, B., Yuan, Z., Qi, Y., & Zhang, Y. (2019). Microstructure and improved hydrogen storage properties of Mg85Zn5Ni10 alloy catalyzed by Cr2O3 nanoparticles. *Journal of Physics and Chemistry of Solids*, *134*, 295–306. https://doi.org/https://doi.org/10.1016/j.jpcs.2019.06.015

Zhang, H. L., Liang, S. T., Luo, M. T., Ma, M. G., Fan, P. P., Xu, H. B., … Zhang, Y. (2014). Preparation and color performance control of Cr2O3 green pigment through thermal decomposition of chromium hydroxide precursor. *Materials Letters*, *117*, 244–247. https://doi.org/10.1016/j.matlet.2013.12.010

Zhang, R., Chang, Q.-Y., Ma, F., Zeeshan, M., Yang, M.-L., Sui, Z.-J., … Zhu, Y.-A. (2022). Enhanced catalytic performance of transition metal-doped Cr2O3 catalysts for propane dehydrogenation: A microkinetic modeling study. *Chemical Engineering Journal*, *446*, 136913. https://doi.org/https://doi.org/10.1016/j.cej.2022.136913

Zhao, C., & Chen, W. (2019). A review for tannery wastewater treatment: some thoughts under stricter discharge requirements. *Environmental Science and Pollution Research*, *26*(25), 26102–26111. https://doi.org/10.1007/s11356-019-05699-6

Zhao, P., Zhao, H., Yu, J., Zhang, H., Gao, H., & Chen, Q. (2018a). Crystal structure and properties of Al2O3-Cr2O3 solid solutions with different Cr2O3 contents. *Ceramics International*, *44*(2), 1356–1361. https://doi.org/https://doi.org/10.1016/j.ceramint.2017.08.195

Zhao, X., Zhang, Y., Qiu, P., Wen, P., Wang, H., Xu, G., & Han, Y. (2018b). C-doped Cr2O3/NaY composite membrane supported on stainless steel mesh with enhanced photocatalytic activity for cyclohexane oxidation. *Journal of Materials Science*, *53*(9), 6552–6561. https://doi.org/10.1007/s10853-018-1997-x

Zhou, Y., Ma, J., Gao, D., Li, W., Shi, J., & Ren, H. (2018). A novel chrome-free tanning approach based on sulfonated tetraphenyl Calix[4]resorcinarene: Preparation and application. *Journal of Cleaner Production*, *201*, 668–677. https://doi.org/https://doi.org/10.1016/j.jclepro.2018.07.196

BIOGRAFÍAS

Carlos, Medina, is Professor at Escuela Superior Politécnica de Chimborazo (ESPOCH), Ecuador, since 2015. He obtained his master's degree in chemistry in 2013 at the University of Navarra, Spain. He has participated in the National and International Congresses and has published articles indexed in SCOPUS on research topics on materials and nanomaterials focused on water treatment and the environment. Decontamination, use of catalysts in polymer pyrolysis, and other topics. He is part of a research programme in collaboration with national and international institutions and universities.

Alexis Patrice, Debut, obtained his Ph.D. in 2000 from the University of Lille, France. He has been a Professor at the University of the Armed Forces (ESPE) since 2008. He has experience in the characterization of nanomaterials at the Centre for Nanoscience and Nanotechnology. He has conducted several research projects in collaboration with national and international institutions and universities. He has published more than 90 articles indexed in SCOPUS, and has more than 10 patents.

Jorge, Silva, is Professor at Escuela Superior Politécnica de Chimborazo (ESPOCH), Ecuador. He has PhD in Chemistry from the Universidad Santiago de Chile. He has several publications in national and international journals and has participated in several research projects. He is the director of the Advanced Materials Research Group (GIMA) at ESPOCH.

Julio, Gallegos, is Chemist graduated at Escuela Superior Politécnica de Chimborazo, Ecuador in 2023. He has participated in projects of the Advanced Materials Research Group GIMA of ESPOCH, which are dedicated to the study of materials at the nanoscale with innovative potential.

Kerlyn, Vicuña is Chemist graduated at Escuela Superior Politécnica de Chimborazo, Ecuador in 2023. He has participated in projects of the Advanced Materials Research Group GIMA of ESPOCH, which are dedicated to the study of materials at the nanoscale with innovative potential.

Paul, Palmay, is Professor in Thermodynamic at Escuela Superior Politécnica de Chimborazo (ESPOCH), Ecuador. He has Ph.D in Thermodynamic Enginering from Rovira i Virgili University (Spain). He has been director of several projects on plastic waste treatment.

Santiago, Carrera, is Professor in Inorganic Chemistry at Escuela Superior Politécnica de Chimborazo (ESPOCH), Ecuador. He has master's degree in chemistry from Universität of Valencia (Spain). She is developing research projects focused on polymers and new materials.